

# Climate and cryosphere cause water yield regime shifts in the Upper Brahmaputra River basin

Hao Li<sup>1,2</sup>, Baoying Shan<sup>3,2</sup>, Liu Liu<sup>1</sup>, Lei Wang<sup>4</sup>, Akash Koppa<sup>2</sup>, Feng Zhong<sup>5,2</sup>, Dongfeng Li<sup>6</sup>, Xuanxuan Wang<sup>1</sup>, Wenfeng Liu<sup>1</sup>, Xiuping Li<sup>4</sup>, and Zongxue Xu<sup>7</sup>

<sup>1</sup>Center for Agricultural Water Research in China, China Agricultural University, Beijing, China

<sup>2</sup>Hydro-Climate Extremes Lab, Ghent University, Ghent, Belgium

<sup>3</sup>Research Unit Knowledge-based Systems, Ghent University, Ghent, Belgium

<sup>4</sup>Institute of Tibetan Plateau Research, Chinese Academy of China, Beijing, China

<sup>5</sup>College of Hydrology and Water Resources, Hohai University, Nanjing, China

<sup>6</sup>Department of Geography, National University of Singapore, Singapore

<sup>7</sup>College of Water Sciences, Beijing Normal University, Beijing, China

**Correspondence:** Liu Liu (liuliu@cau.edu.cn)

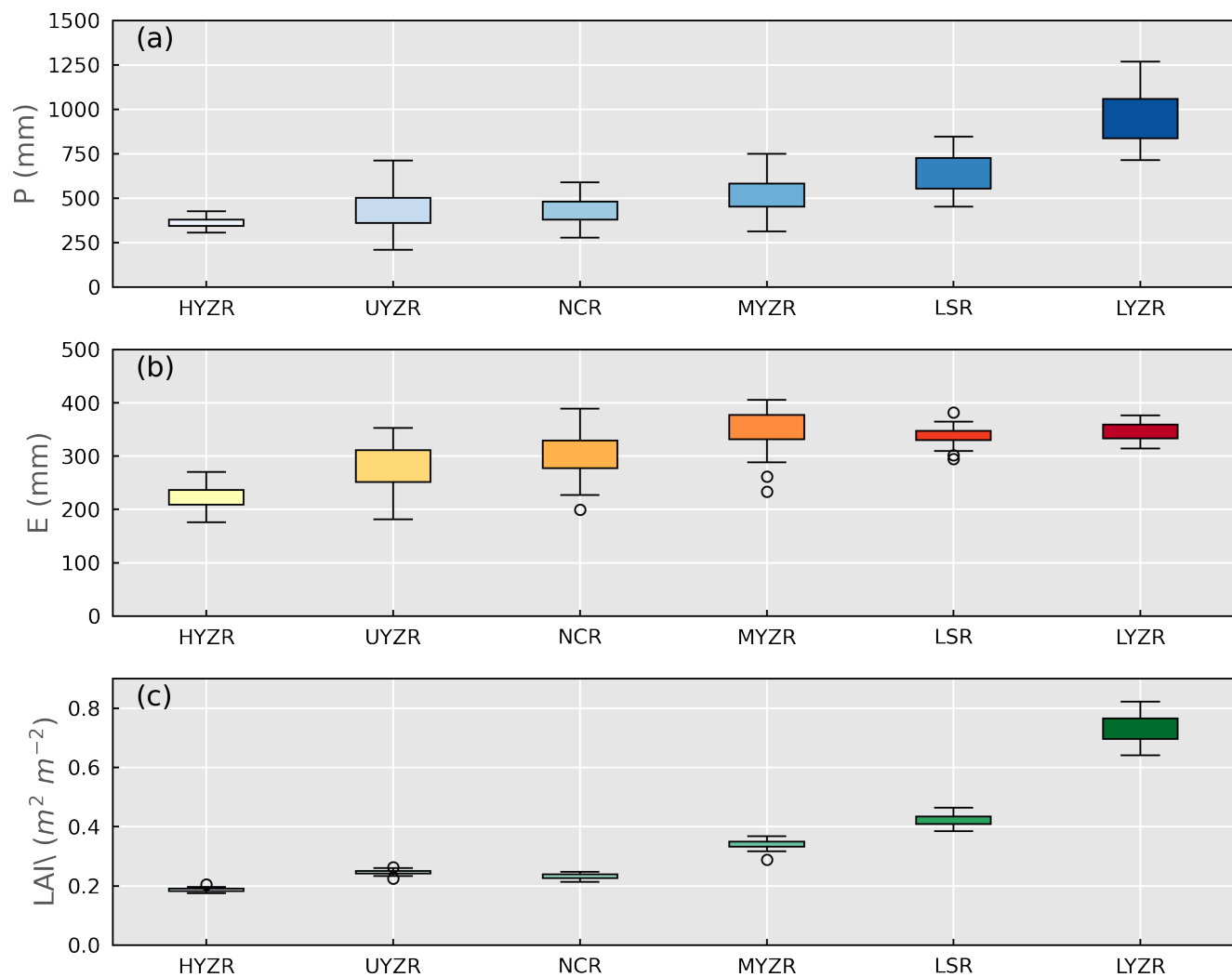


**Figure S1.** The distribution of (a) precipitation (P), (b) evaporation (E), and (c) Leaf Area Index (LAI) during 1982–2013 in the entire UBR basin. Black "x" signals show the mean value.

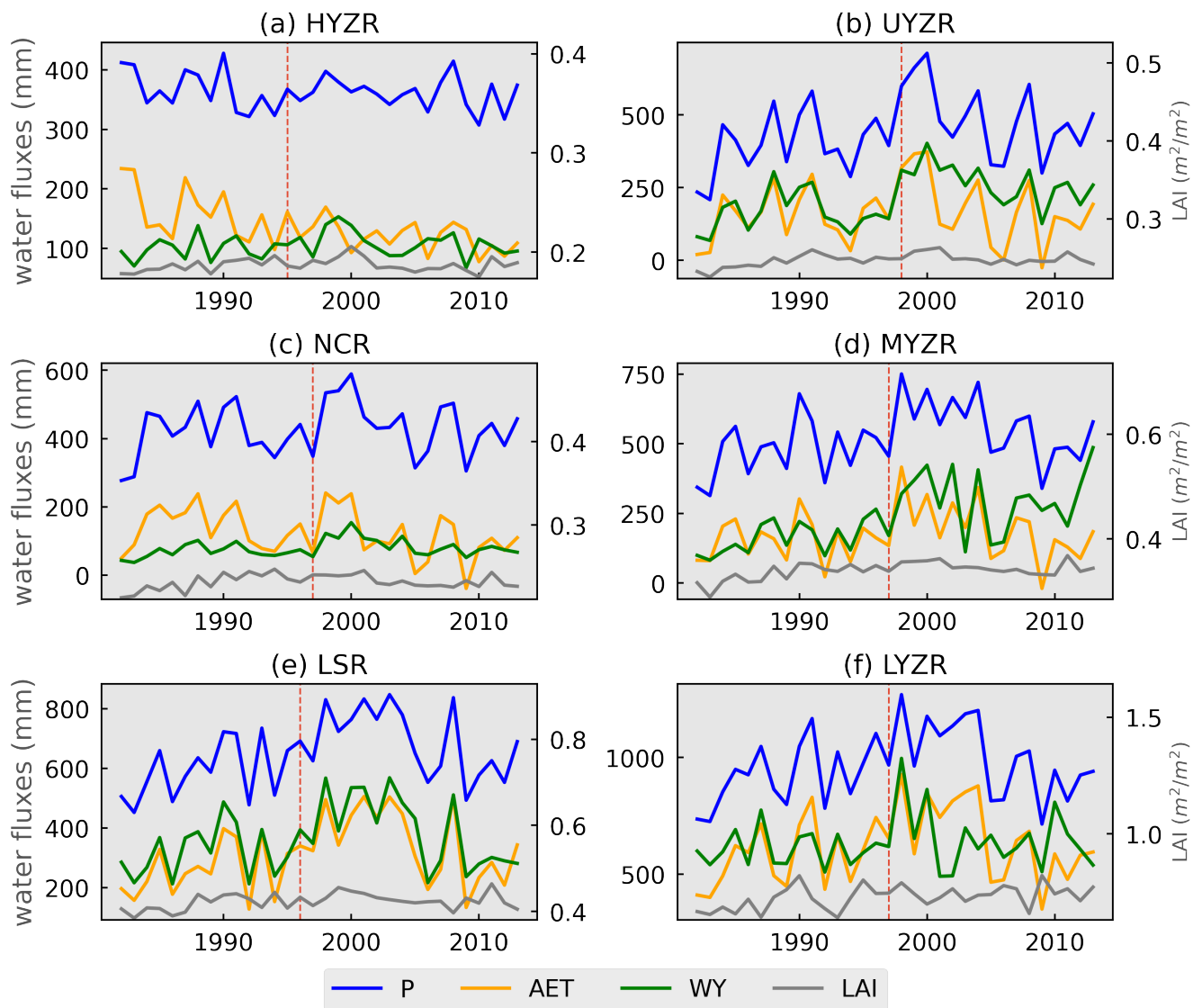


**Figure S2.** The temporal changes of precipitation (P, blue line), evaporation (E, orange line), and water yield (WY, green line) and Leaf Area Index (LAI, grey line) during 1982–2013 in the entire UBR basin. The vertical line indicates the turning point in WY.

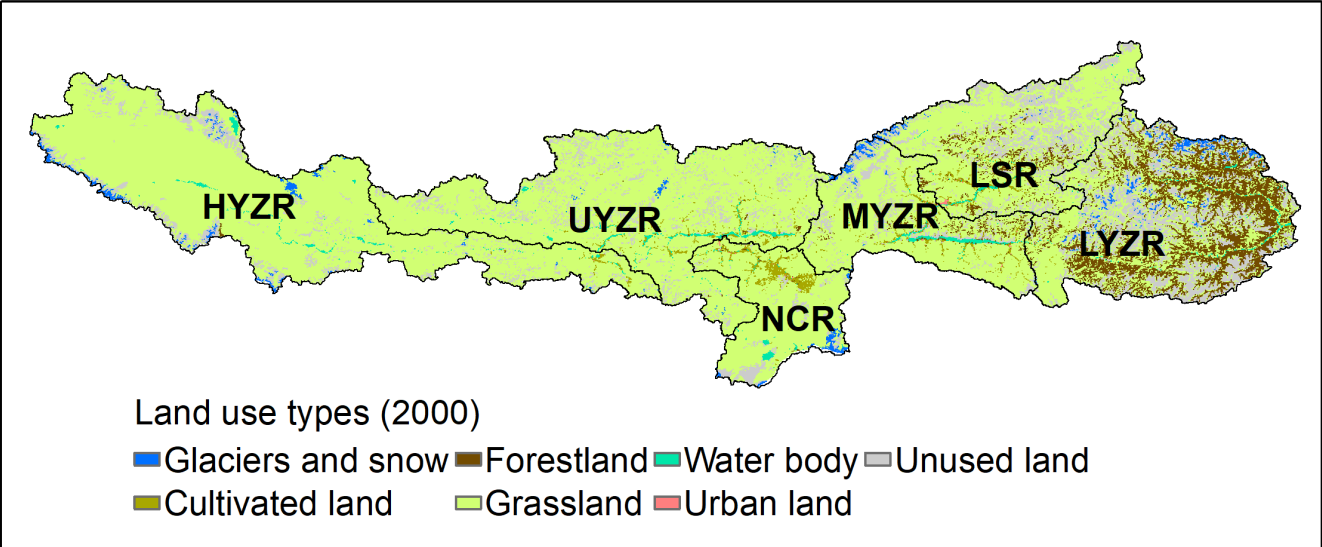


**Figure S3.** The land use types in 2000 in the UBR basin.

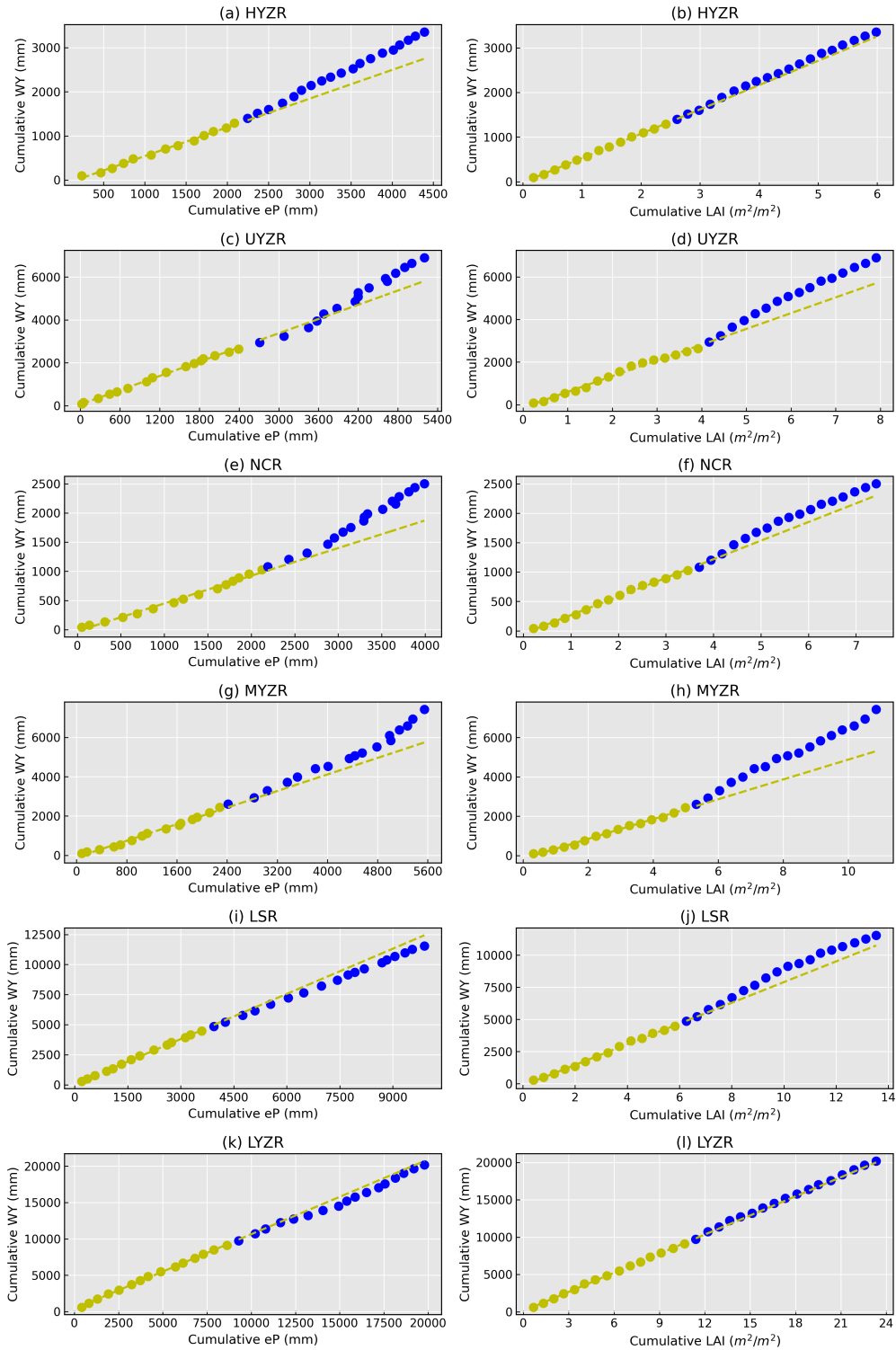


**Figure S4.** Double mass curves in the entire UBR basin. The left panel (a+c+e+g+i+k) shows the double mass curve between cumulative eP (x-axis) and WY (y-axis), and the right panel (b+d+f+h+j+l) shows the double mass between cumulative LAI (x-axis) and WY (y-axis). The color of points represents the period before (yellow) and after (blue)  $T_p$ . The dash line indicates the predictions by inputting cumulative eP or LAI in Equation (2) or (3) in main text.

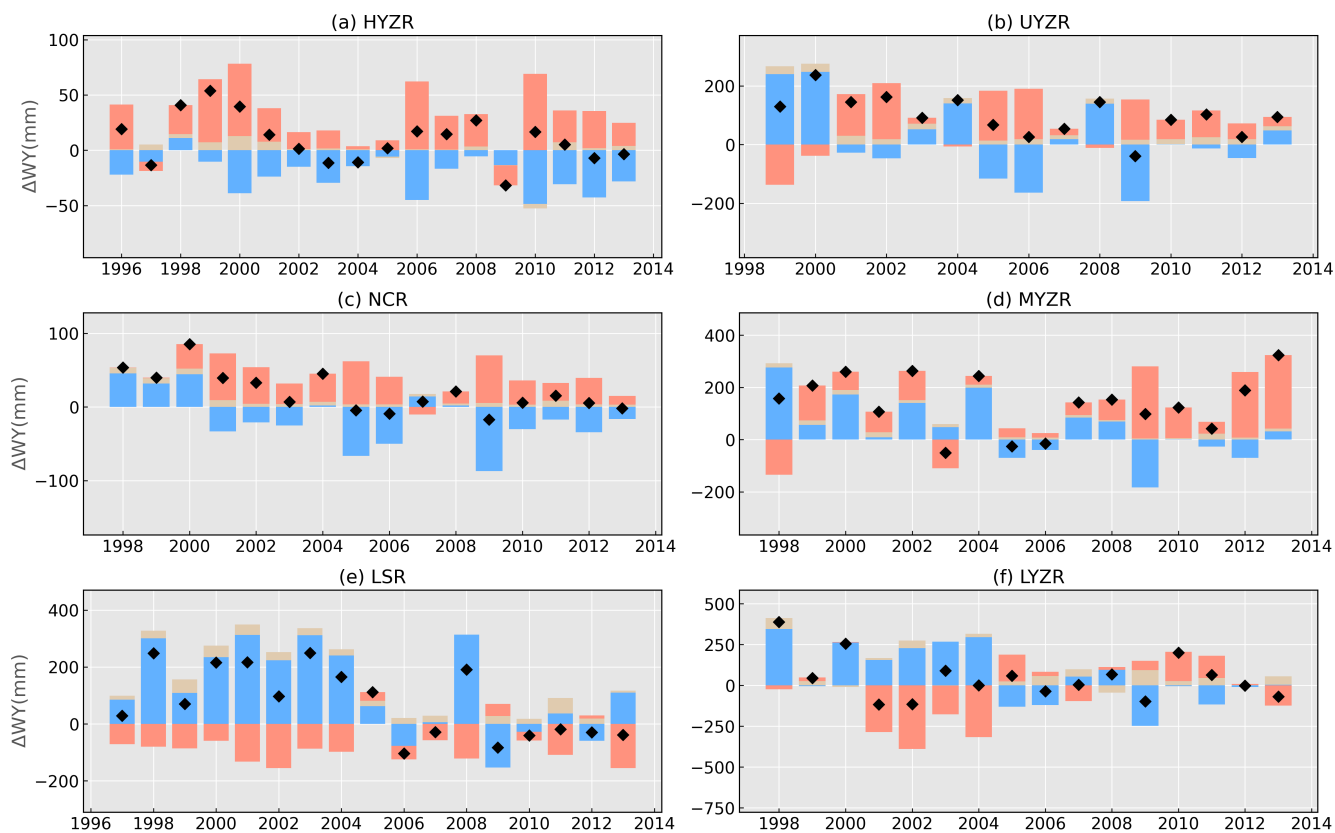


**Figure S5.** Time series after  $T_p$  of total water yield deviation ( $\Delta WY_s(t)$ , black diamond), consisting of water yield deviation from climate ( $\Delta WY_c$ , blue bar), vegetation ( $\Delta WY_v$ , tan bar), and cryosphere ( $\Delta WY_g$ , red bar).

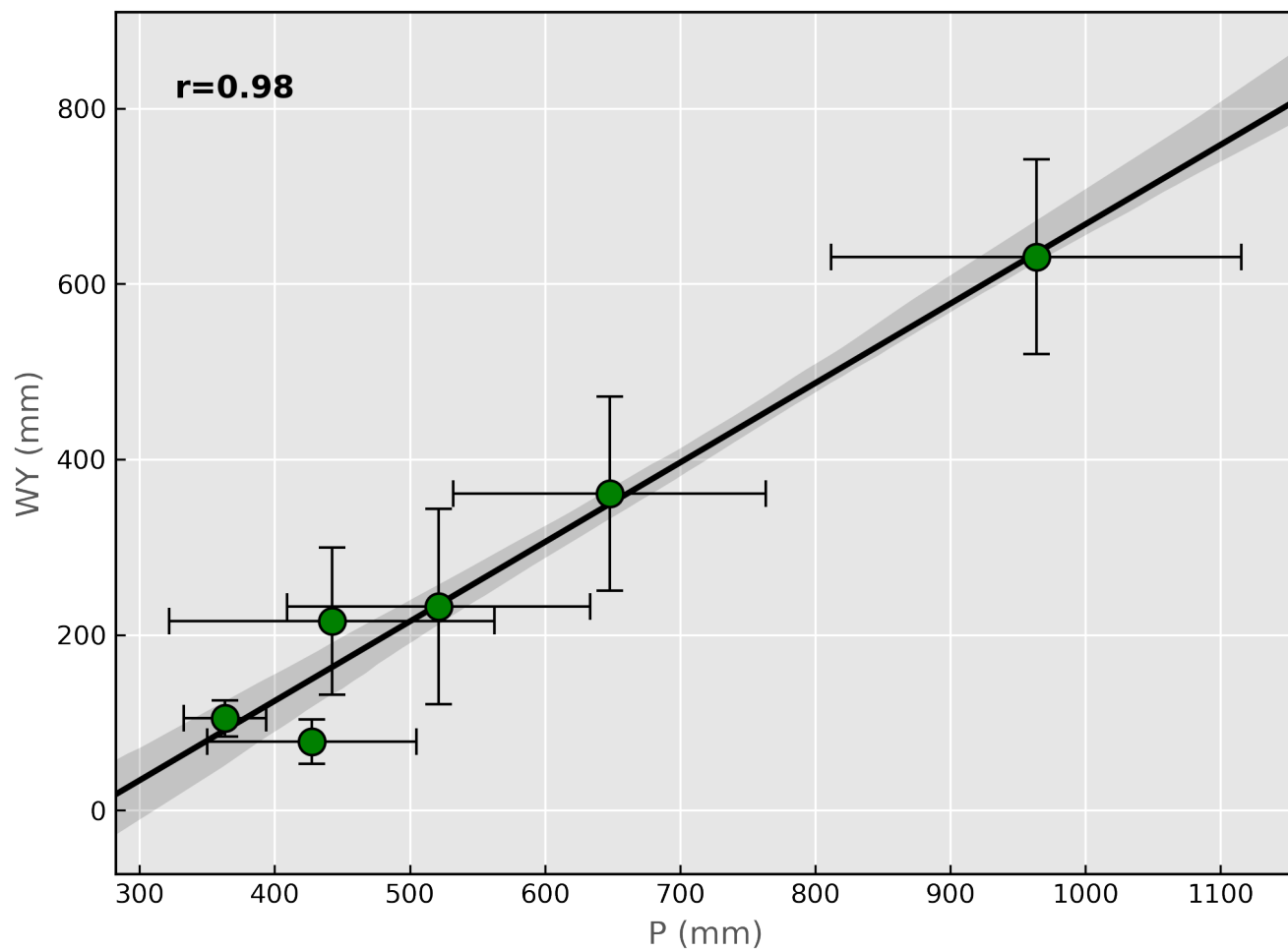


**Figure S6.** The relationship between precipitation (P) and water yield (WY) in the entire UBR basin. The error bar represents one standard deviation. The shading area indicates the 95% confidence interval of the linear fitting.

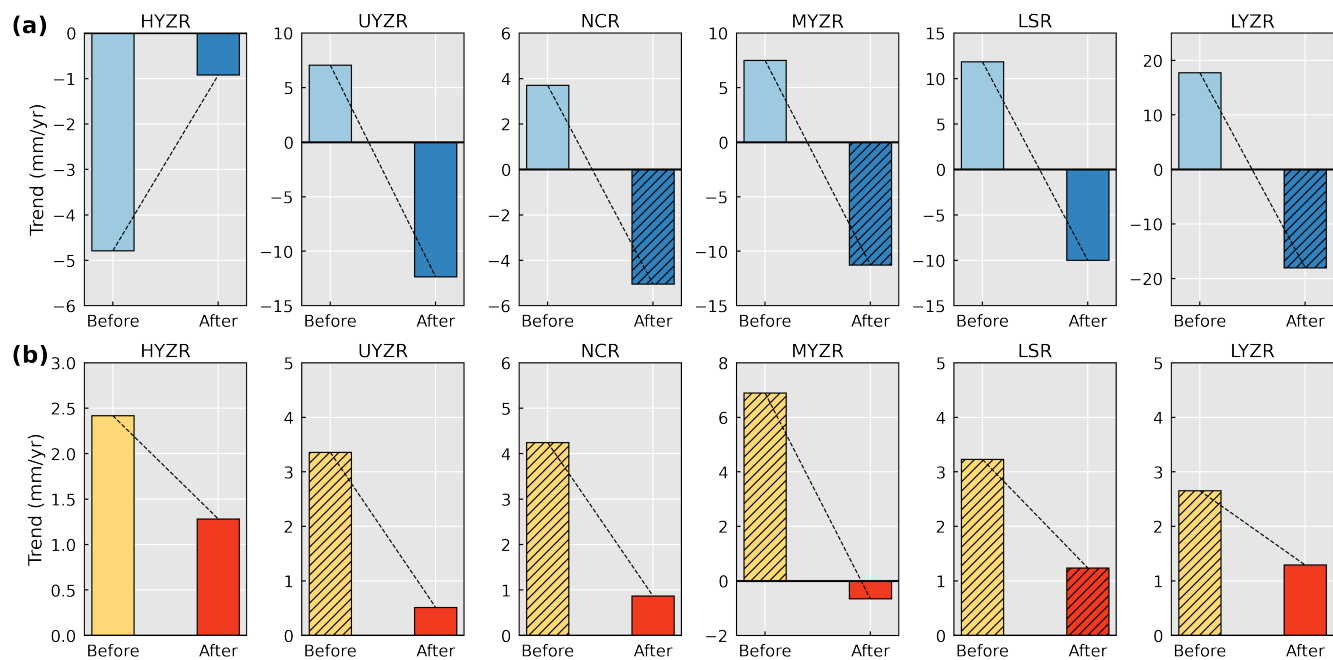


**Figure S7.** Direction of precipitation (a) and evaporation (b) changes. The black hatching represents the statistically significant trend ( $p < 0.05$ ). The color of boxes represents the period before (light color) and after (dark color) Tp.



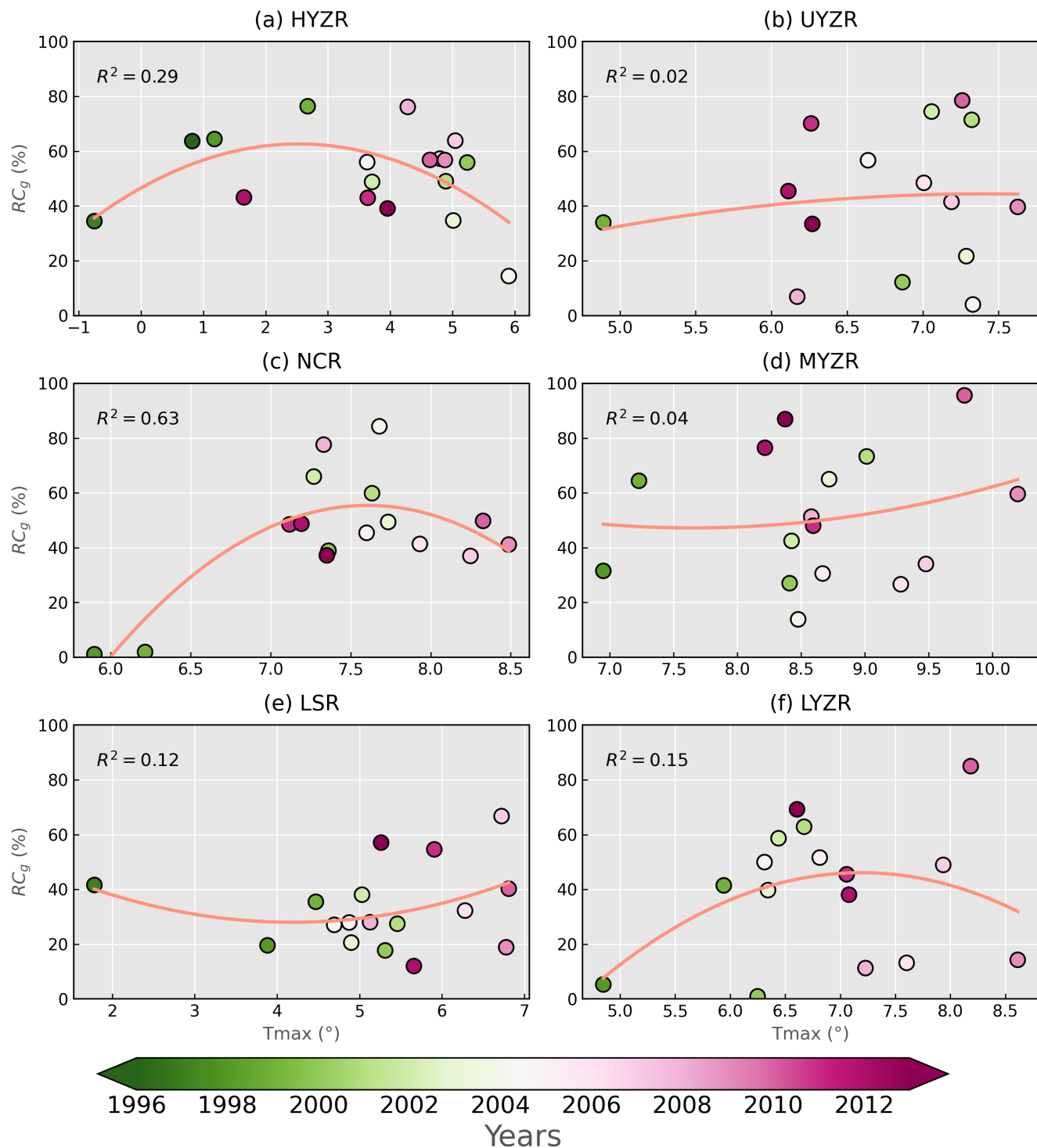


**Figure S8.** The relationship between cryospheric contributions to water yield deviations ( $RC_g(t)$ , see Data and Methods) and annual mean 2 m maximum air temperature ( $T_{max}$ ) using the polynomial fitting. The colorbar indicates the years after  $T_p$  in individual basins. R square here used to evaluate the fitting goodness is labelled in each panel. 9

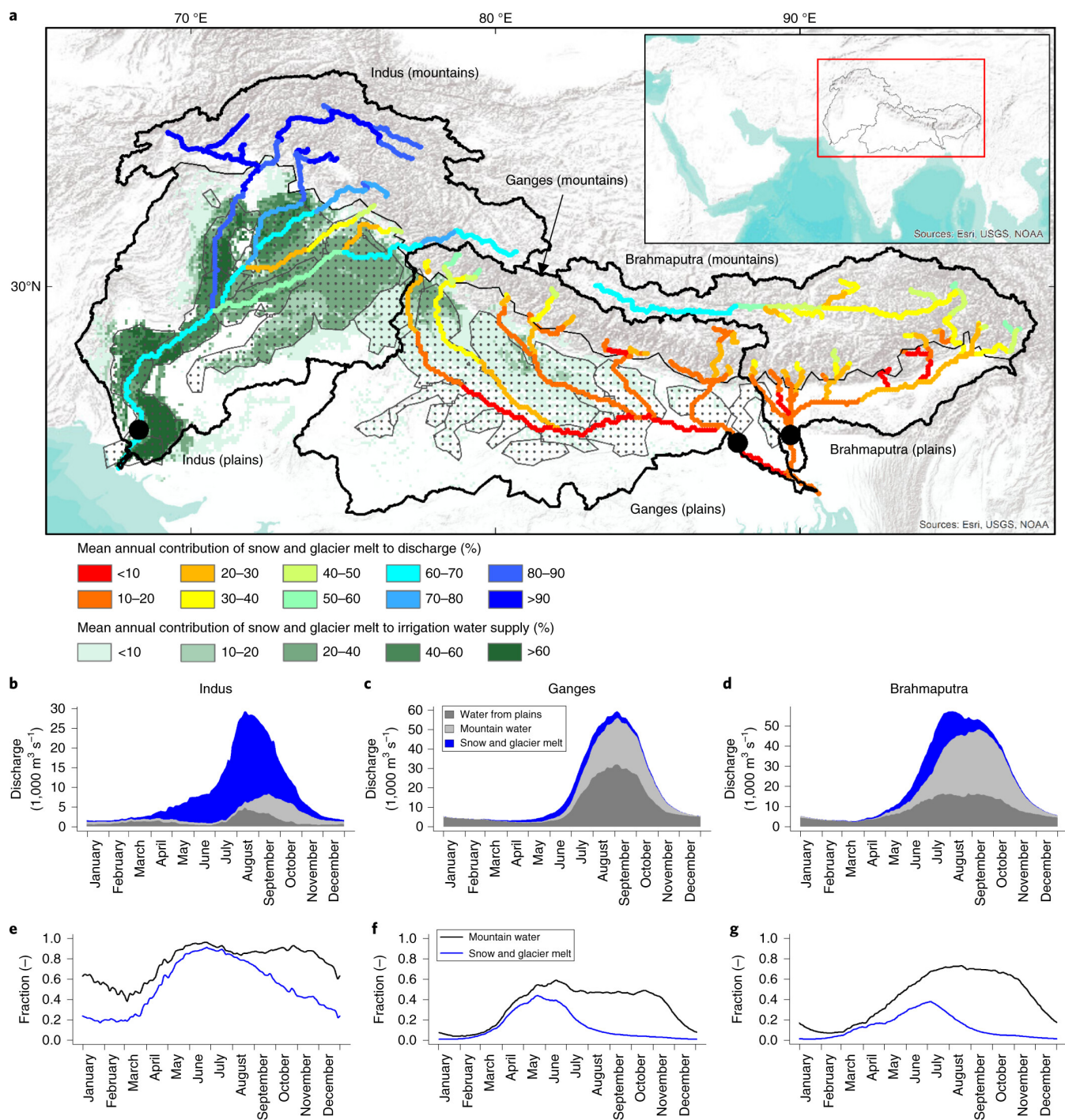


**Figure S9.** The spatially explicit, mean annual contributions of snow and glacier melt to river flow from Biemans et al. (2019).

## References

Biemans, H., Siderius, C., Lutz, A., Nepal, S., Ahmad, B., Hassan, T., von Bloh, W., Wijngaard, R., Wester, P., Shrestha, A., et al.: Importance of snow and glacier meltwater for agriculture on the Indo-Gangetic Plain, *Nature Sustainability*, 2, 594–601, 2019.